Nanostructured Acid/Base Materials Via Nitridation

Abdelrahman Ali H. Ali[1], Robert Mokaya[2]

[1]Departemetn of Chemistry, Faculty of Science, Sirte University, Sirte, Libya.
nanochemist13@su.edu.ly, Phone No: 00218 91 3810953
[2]School of Chemistry, University of Nottingham, University Park, Nottingham NG7 2RD, U.K.
r.mokaya@nottingham.ac.uk

Abstract: Recently, porous templated materials have attracted significant attention owing to their unique properties and their potential applications. The ease of preparation and control of the surface functionality (basic and/or acid/base) of the mesoporous aluminosilica oxynitride materials makes them attractive as alternative solid acid/base catalysts, especially for large-molecule transformations. Mesoporous silica materials are currently the subject of intense research interest. Herein, the method of preparation and structure characterization of composite micro/mesoporous crystalline materials consisting of novel solid acid-base mesoporous aluminosilica oxynitride materials been presented. Experiments been performed using previously reported procedures to this purpose. The preparation procedure involves two-steps: i) formation of a mesostructured material composed of zeolite aluminosilicate micro/mesoporous material by a crystallisation process, varying the aging time between 2 – 16 h and ii) the calcined samples been subjected to high temperature nitridation, i.e. treatment with ammonia at elevated temperature. The produced nanostructured acid/base micro/mesoporous aluminosilica oxynitride materials was investigated using a variety of techniques including powder X-ray diffraction (XRD), nitrogen sorption, thermo-gravimetrical analysis (TGA), X-ray fluorescence (XRF) and elemental analysis. Results showed the possibility of generating composite materials of a cubic MCM-48 phase and zeolite ZSM-5. The textural properties of the composite materials confirmed that the materials exhibit various levels of micro/mesoporous structure with relative narrow pore size distribution. The maintenance of the structure ordering after a nitridation treatment were found depends on the conditions of the treatment with ammonia.
[Abdelrahman Ali H. Ali. Nanostructured Acid/Base Materials Via Nitridation**.** *J Am Sci* 2018;14(5):18-24]. ISSN 1545-1003 (print); ISSN 2375-7264 (online). http://www.jofamericanscience.org. 4. doi:10.7537/marsjas140518.04.

Keywords: Nanostructured, Acid/Base Materials, Mesoporous, Cubic MCM-48, Zeolite ZSM-5.

Introduction

One of the most significant current discussions in the scientific and technological areas is the term 'Nano' (Nanoscience and Nanotechnology). Mesoporous silica materials are currently the subject of intense research interest. The ease of preparation and control of the surface functionality (basic and/or acid/base) of the mesoporous aluminosilica oxynitride materials makes them attractive as alternative solid acid/base catalysts especially for large-molecule transformations. There is a need for a single synthetic method that allows the control of the structural and textural characteristics of the materials in order to generate porous materials with appropriate morphology, and well-defined and optimised textural properties for their subsequent applications. This work mainly focused on the syntheses and applications of nanomaterial. Several works been repeated focused on the porosity of materials and the applications of ordered mesoporous aluminosilicate materials.[1-6]

Experimental Section

Materials

A 10% Tetrapropylammonium hydroxide (TPAOH) and 98+% cetyltrimethyl-ammonium bromide (CTAB) were obtained from Acros, sodium hydroxide was supplied from Fisher Scientific, aluminium isopropoxide (AIP) 98+% was obtained from Aldrich, and tetraethyl orthosilicate (TEOS) with a purity of ≥ 98% from Fluka. All materials were used as received.

Synthesis of Materials

The Na-ZM48 materials were prepared hydrothermally fallowing repeated procedure.[3, 7] The precursor zeolite gel species (with ZSM-5 primary units) was synthesized by mixing TPAOH, AIP, and TEOS. The mixture was aged at 100°C at different aging times (2 – 16 h) and allowed to cool down to room temperature. The resulting preformed zeolite species were then added to a surfactant cetyltrimethylammonium bromide (CTAB) template solution containing sodium hydroxide. The molar ratio of the resulting synthesized gel was 1: 0.12: 0.5: 0.0125: 118 (TEOS: CTAB: OH: Al: H_2O respectively). After stirring for 2 h at room temperature, the synthesized gel was transferred to a Teflon-lined autoclave and heated at 150 °C for 8 h. After cooling to room temperature, the resulting as-synthesized solid product firstly filtered direct at room temperature and then calcined in air at 550 °C for 6h. The samples thus prepared were designated as ZM48Bx, where x is the

aging time (i.e. x= 2, 3, 4, 6, 8, 16 h). The calcined Na-containing samples were then subjected to characterization.

Sample Nitridation

The samples ZM48Bx (x= 4, 8, 16) were nitrided following an established procedure, [4, 8-9] as illustrated schematically in Figure 1. The calcined zeolite aluminosilicate materials were then subjected to a high temperature nitridation process (i.e. treatment with ammonia at elevated temperature). The typical procedure consisted of placing ca. 0.3 g of ZM48Bx in an alumina boat and introducing it into a flow-through tube furnace. The tube furnace was purged by Nitrogen gas (N_2) for 30 min, and then further purged with ammonia (NH_3) for another 30 min. A NH_3 flow rate of 100 mL/min was fixed and the temperature of the furnace was raised at a ramp rate of 5°C/min to 950 - 1150ºC and then maintained for 20 h under the NH_3 atmosphere. The furnace was then cooled to ca. 100°C under NH_3 and then switched to N_2 until it cooled to room temperature. The resulting nitrided samples were denoted NHy-ZM48Bx (y = 1 for 950 °C, 2 for 1050 °C and 3 for 1150 °C).

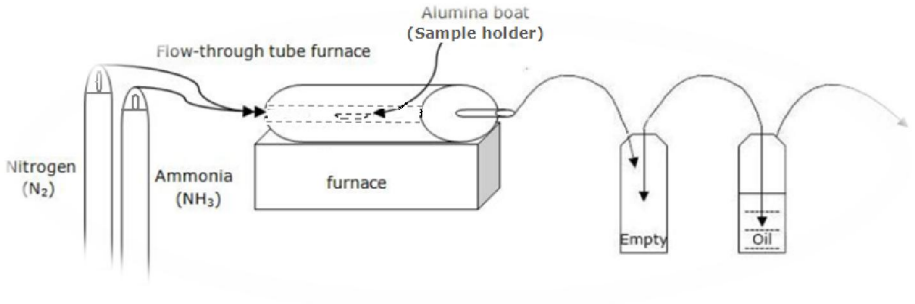

Figure 1 Schematic diagrams illustrating the nitridation procedure of ZM48Bx samples.

Powder X-Ray Diffraction Technique (XRD)

Powder XRD measurements were performed on PANalytical X'Pert powder diffractometer with Cu-Kα radiation (λ= 1.5418 Å), operating at 40 kV and 40 mA and using a 0.025˚ step size and ca. 40 s step time for values of 2θ = 0.65° - 50°. Two types of sample holders (stainless steel and silicon coated zero background holders) were used for powder samples preparation.

X-Ray Fluorescence (XRF).

A Phillips MiniPal PW4025 XRF instrument been utilized to determine the elemental composition of the samples. The instrument was pre-calibrated to give the Si/Al ratio. Five runs used to determine the percentage average with the aim of reducing the experimental error associated with single XRF measurements.

Thermo-Gravimetric Analysis (TGA)

TGA analysis was done in a TA Instruments SDT Q600 Analyser with an automated horizontal thermo-balance. The samples were heated in alumina pans (sample holder) at a ramp rate of 10°C/min to 1000°C in static air condition.

Nitrogen Physisorption Isotherm Analysis (N_2).

A Micrometrics ASAP 2020 volumetric sorpometer was used to determine the textural properties of the synthesized samples via N_2-physisorption isotherms at -196 °C. Before analysis, ca. 0.2 g of each individual sample was degass overnight at 150 °C under high vacuum. The surface area was estimated using the BET method based on nitrogen adsorption data in the relative pressure range P/P_o = 0.06 - 0.25.[10] The total pore volume was calculated from the amount of liquid nitrogen adsorbed at P/P_o ca. 0.99.[2,5,11] The pore size distribution was determined by non-local density functionaltheory (NLDFT) assuming slit-like pore geometry and by the BJH method. [5,6]

Elemental microanalyzer (CHNs)

The nitrogen content of the nitrided sample was obtained using a CHN_S Analyzer model CE-440 made of Exeter Analytical, Inc. (EAI).

Results and Discussion

Calcined Materials

Physicochemical characterization of the calcined materials was assessed using powder XRD. Figure 2. Shows the powder XRD patterns of ZM48Bx materials, where x is the aging time in hours (x = 2, 3, 4, 6, 8 and 16 h). All materials display distinctive XRD patterns, which are reproducible for any given synthesis conditions. They show a (211) diffraction peak at 2Θ~ 2.5˚, along with a lower intensity peak at 2Θ ~ 4.7˚, which are attributed to an ordered cubic (Ia3d) MCM-48 structure. Several other peaks were identified in the 2Θrange = 7-10˚ and 20-30˚. These peaks were corresponded to the zeolite ZSM-5 phase.[3] This result indicates that the formed material is composed of a cubic MCM-48 phase and ZSM-5 zeolite. The d_{211} spacing is in the range of 3.3-3.6 nm, as shown in Table 1. The XRD pattern of the sample ZM48B2, that was aged for only 2 h, shows a very

intense and narrow (211) reflection, which corresponds to a well ordered cubic MCM-48 structure.[3, 12-15] However, peaks corresponding to the ZSM-5 zeolite are also identified, contrary to what Xia and Mokaya had previously reported.[3]

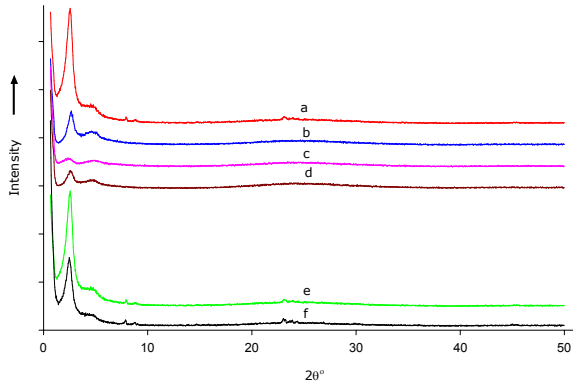

Figure 2. Powder XRD patterns for calcined Na containing samples aged at 100 °C for several hours (2 – 16h) (a) $ZM48B_2$, (b) $ZM48B_3$, (c) $ZM48B_4$, (d) $ZM48B_6$, (e) $ZM48B_8$ and (f) $ZM48B_{16}$.

The variation of the aging time from 2 h to between 3 and 6 h (samples $ZM48B_3$, $ZM48B_4$ and $ZM48B_6$, respectively), led to the disappearance of the zeolite phase and the progressive destruction of the MCM-48 phase, as shown by the decrease of the intensity of the (211) peak. However, it is remarkable that for the longest aging times, 8 and 16 h (samples $ZM48B_8$ and $ZM48B_{16}$, respectively), the intensity of the MCM-48 phase peaks increases instead of dropping, as expected, and zeolite ZSM-5 phase is formed again.

The textural properties of the materials were evaluated by physisorption of N_2 at -196°C. Figure 3. Shows the N_2 sorption isotherms of the materials and the related textural properties are summarized in Table 1. All samples exhibit type IV isotherm with a well-developed capillary condensation step in the relative pressure (P/P_o) range 0.2 - 0.4. This indicates that they all have a uniform mesoporous structural ordering. It is noteworthy that samples $ZM48B_2$, $ZM48B_8$ and $ZM48B_{16}$, which have a considerably high content of zeolitic material, still exhibit a high degree of mesoporous structure. This findings confirm that all the materials have a well-developed mesoporous structure with relative narrow pore size distributions.

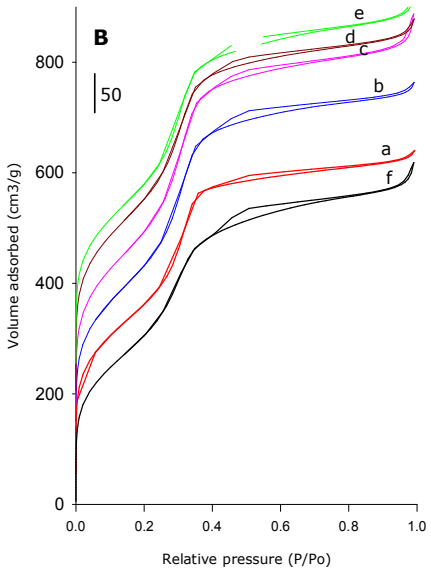

Figure 3. Nitrogen sorption isotherms for calcined Na containing samples aged at 100 °C for several periods of time in the 2 – 16h range: (a) $ZM48B_2$, (b) $ZM48B_3$, (c) $ZM48B_4$, (d) $ZM48B_6$, (e) $ZM48B_8$ and (f) $ZM48B_{16}$.

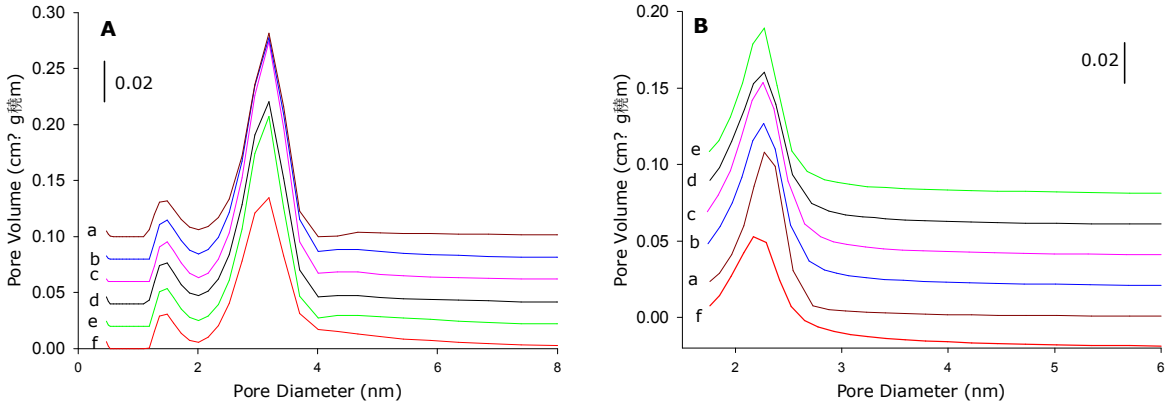

Figure 4; pore size distribution curves of the calcined ZSM-5/MCM48 composites materials (A) NLDFT adsorption data and (B) BJH adsorption data; (a) $ZM48B_2$, (b) $ZM48B_4$, (c) $ZM48B_3$, (d) $ZM48B_4$, (d) $ZM48B_6$, (e) $ZM48B_8$, and (f) $ZM48B_{16}$.

Table 1. Textural properties and elemental composition of the calcined sodium containing samples.

Sample	Aging time (°C/h)[a]	Si/Al ratio	d_{211}spacing (nm)	Surface area (m^2g^{-1}) [b]	Pore volume (m^3g^{-1}) [c]	Pore size maxima (nm) [d]	Pore size maxima (nm) [e]
$ZM48B_2$	2	16.6	3.40	1160(304)	0.91(0.32)	2.3	1.5/3.2
$ZM48B_3$	3	15.5	3.35	1250(0)	1.03(0.15)	2.3	1.5/3.2
$ZM48B_4$	4	15.9	3.40	1297(0)	1.14(0.11)	2.3	1.5/3.2
$ZM48B_6$	6	15.9	3.35	1318(242)	1.05(0.28)	2.3	1.5/3.2
$ZM48B_8$	8	18.2	3.51	1237(316)	1.03(0.33)	2.3	1.5/3.2
$ZM48B_{16}$	16	17.4	3.64	1144(90)	0.96(0.15)	2.2	1.5/3.2

[a] Aging time of the precursor zeolite species. [b] The values in parentheses are the micropore surface area. [c] The values in parentheses are the micropore volume. [d] Maxima of BJH pore size distribution. [e] Maxima of DFT pore size distribution.

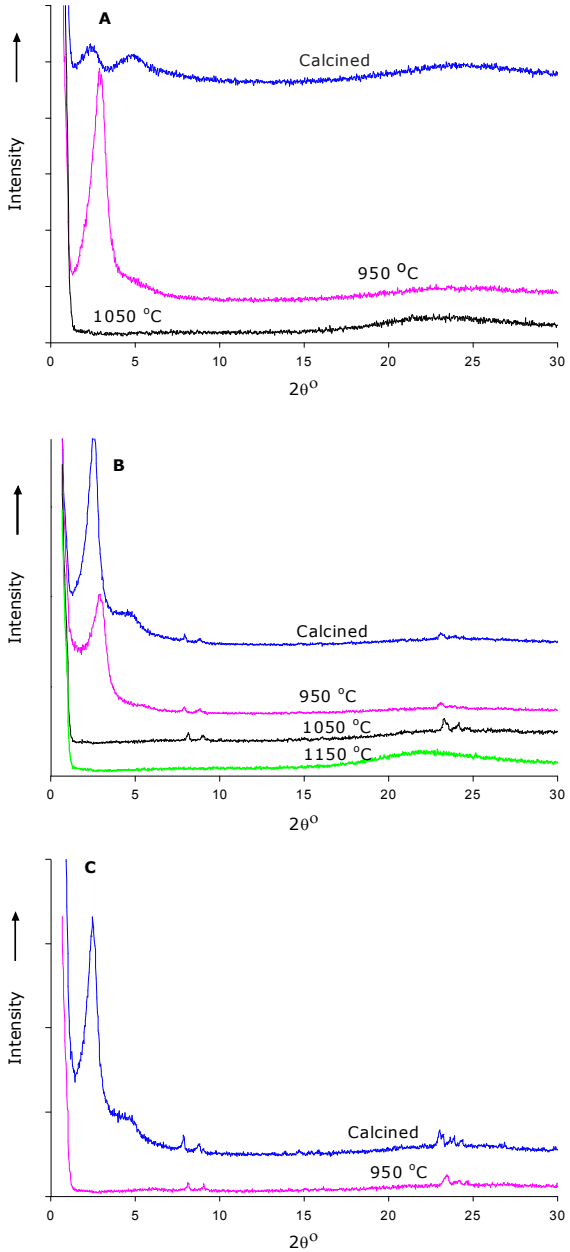

Figure 5. Powder XRD patterns of of (A) NH_y-$ZM48B_4$, (B) NH_y-$ZM48B_8$, and (C) NH_y-$ZM48B_{16}$ before and after nitridation procedures at various temperature degrees: 950 °C, 1050 °C, and 1150 °C respectively.

The pore size distribution of all the studied materials was determined by means of two models using the adsorption data, i.e. NLDFT and BJH, and is presented in Figure 4. It is noteworthy that, even though the DFT model applied to the N_2 sorption isotherm can overestimate the pore size [16], it is still useful in present circumstance of a comparison analysis [17]. It possesses the advantage over the BJH model, which is only applicable to mesopores, that it can be applied to materials having both micropores and mesopores. Thus, the DFT curves (Figure 4A) shows bimodal pore size distributions for all the samples, with one of the pore systems centred at ca. 1.5 nm and the other at 3.2 nm. On the other hand, the BJH curves (Figure 4B) display a single peak at 2.2 nm for all the samples as well. The pore size distribution data suggest that all the materials exhibit micro/meso-porosity, which is in an excellent agreement with the XRD data shown in Figure2.

The textural data presented in Table 1 show that the increase of the aging time between 2 and 6 h leads to rise in the surface area from 1160 to 1318 m^2g^{-1}. However, for longer aging times, it decreases. The highest surface area and pore volume correspond to the sample aged for 6 h ($ZM48B_6$), whereas the sample aged for the longest time, 16 h ($ZM48B_{16}$), possesses the lowest values of both parameters.

Thermo-gravimetric analysis (TGA) was used to investigate the removal of the organic additives/templates (i.e., CTAB and TPAOH). All the studied samples display a weight loss below ~110ºC, which is due to desorption of water, and another between 110 and 300 °C, which corresponds to the thermal decomposition of the organic additives. This last weight loss exhibits two different weight loss rates, one in the 110 - 200˚C range and another in the 200 – 300˚C range, which are caused by the thermal decomposition of the different organic additives, CTAB and TPAOH, respectively.

Well-established X-ray fluorescence (multi-elemental analysis) technique with the associated Minipal software was used to determine Si/Al ratio. The accuracy of results was improved by repeated quantification. The elemental composition of the target materials are given in Table 1. Samples aged for 3 – 6 h have the same Si/Al ratio, ~ 16, whereas the rest of

the samples have a Si/Al ratio in the ca. 17-18 range. The sample aged for 8 h ($ZM48B_8$) possesses the highest Si/Al ratio of all the materials. This indicates that the Al content decreases at longer aging times. Overall, the Si/Al ratios point out the proportion of Al compared to Si that was retained in the solid products.

Oxy-Nitrided Samples

The nitridation reaction occurs according to the flowing schemes:

$$\equiv Si\text{-}OH + NH_3 \longrightarrow \equiv Si\text{-}NH_2 + H_2O$$

and/or

$$\equiv Si\text{-}O\text{-}Si\equiv + NH_3 \longrightarrow \equiv Si\text{-}NH\text{-}Si\equiv + H_2O$$

or $\equiv Si\text{-}NH_2 + \equiv Si\text{-}OH$

Figure 5. Shows the powder XRD patterns before and after nitridation at various temperatures for samples $ZM48B_4$, $ZM48B_8$ and $ZM48B_{16}$. There is a clear decrease of the intensity of the (211) reflection as the nitridation temperature increases, which indicates the progressive destruction of the cubic MCM-48 phase with the increase of the nitridation temperature. For the samples aged for 4 and 8 h, the cubic phase completely collapses for T ≥ 1050 ˚C, whereas for the sample aged for 16 h it disappears at a lower temperature, 950 ˚C. This may be evidence of a higher stability against the nitridation treatment of the MCM48 phase in the samples aged at shorter times. On the other hand, the zeolitic phase present in the samples aged for 8 seems to remain stable after the nitridation treatment up to 1150 ˚C. This means that the temperature at which the treatment with ammonia is performed is a key factor in maintaining the structure ordering throughout nitridation procedure.[8] The basal (d_{211}) spacing (Table 2) shows a falling of ca. 1% related to the calcined materials (Table 1).

Table 2. Textural properties and elemental composition of the aluminosilica oxynitride samples.

Sample	$T_{nitridation}$ (˚C)	Aging time (°C/h)[a]	Si/Al ratio	N content wt%	d_{211} spacing (nm)	Surface area (m^2g^{-1}) [b]	Pore volume (m^3g^{-1}) [c]	Pore size maxima (nm) [e]
NH_1-$ZM48B_4$	950	4	17.0	4.04	3.11	982(784)	0.55(0.32)	1.4/2.3
NH_2-$ZM48B_4$	1050	4	14.9	-	-	68(50)	0.08(0.02)	1.2
NH_1-$ZM48B_8$	950	8	17.6	4.16	3.01	770(586)	0.44(0.24)	1.4/2.3
NH_2-$ZM48B_8$	1050	8	16.3	-	-	265(179)	0.20(0.08)	0.6/1.4/2.2
NH_1-$M48B_{16}$	950	16	16.7	7.99	-	625(381)	0.41(0.16)	1.4/2.3

[a] Aging time of the precursor zeolite species. [b] The values in parentheses are the micropore surface area. [c] The values in parentheses are the micropore volume. [d] Maxima of BJH pore size distribution. [e] Maxima of DFT pore size distribution.

The textural properties (surface area, pore volume, and pore size) are summarized in Table 2. It can be seen that the samples nitrided at 950˚C display a characteristic type IV isotherm with a sharp capillary condensation step, which indicates uniform pores, for $P/P_0 < 0.2$ and there is nearly no hysteresis. A clear displacement of the capillary condensation step to lower relative pressures; is therefore observed after the nitridation treatment at 950˚C, which suggests a decrease in the pore size. This were confirmed by the pore size distributions of the samples (Figure 6), which show a decrease in the mesopore size from 3.2 nm (Table 2) to 2.3 nm (Table 2). This is consistent with previous results which indicate that there are two main factors contributing to the decrease of pore size: firstly, thermal treatment at high temperature results in the contraction of the mesoporous silica network and secondly, the nitridation process results in a significant increase of the pore wall thickness,[9] After rising the nitridation temperature from 950 to 1050 °C, the capillary condensation step disappears, the isotherm being type I, typical of microporous materials. However, the broad isotherm knee in sample NH_2-$ZM48B_8$ suggests the existence of small mesopores. This been supported by the DFT PSD curve shown in Figure 6B, which show the existence of a certain proportion of pores ~ 2 nm.

Figure 6. Shows the pore size distribution curves of the nitrided samples determined via DFT (Figure 6A, 6B and 6C) and BJH (Figure 6D, 6E and 6F) models using adsorption data. DFT curves display bimodal pore size distribution at ca. 1.4, and 2.3 nm for all the samples nitrided at 950 ˚C. However, on increasing the temperature from 950 to 1050°C the DFT curves exhibit monomodal distributions at ca. 1.2 for NH_2-$ZM48B_4$ and trimodal at ca. 0.6, 1.4, and 2.2 nm for NH_2-$ZM48B_8$. On the other hand, as previously mentioned, the BJH model is only for mesoporous materials, which explains the shape of the curves in Figures 6D, 6E and 6F, as the samples possess pores just in the limit between micropores and mesopores.

We note that the surface area of the nitrided materials (Table 2) decreases to a great extent at high temperature treatment in ammonia, as earlier has been observed for other type of porous materials.[9] Thus, the sample $ZM48B_4$ nitrided at 1050 °C (i.e. NH_2-$ZM48B_4$) retains only ca. 5% of the surface area of the calcined material. However, the sample NH_2-$ZM48B_8$ possesses ca. 21% of the surface area of the calcined one at same conditions. Nevertheless it should be noted that when the sample $ZM48B_8$ was nitrided at a temperature higher than 1150 °C, the surface area was

almost null, indicating a complete collapse of the structure, which agrees well with the XRD spectra in Figure 5B, where no XRD peaks can be identified.

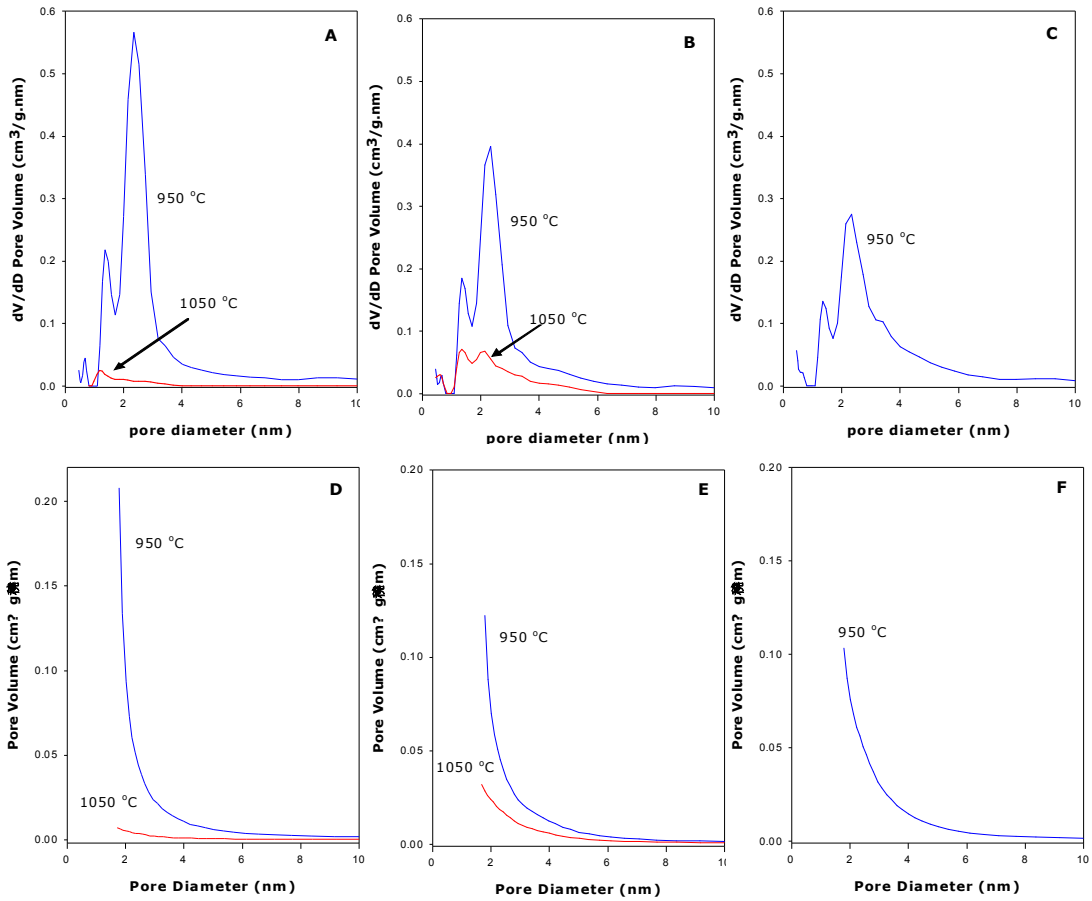

Figure 6. Pore size distribution curves of NH_y-$ZM48B_4$ (A and D), NH_y-$ZM48B_8$ (B and E), and NH_y-$ZM48B_{16}$ (C and F) nitrided at 950 °C and 1050 °C, determined via DFT (A, B and C respectively) and BJH (D, E and F respectively) models using adsorption data.

The elemental composion (Si/Al ratio and N content) data for the aluminosilica oxynitrided materials is given in Table 2. It can be seen that the Si/Al ratio decreases by ca. 3-4% for most of the samples when nitrided at 950 °C. However, for the sample $ZM48B_4$, the Si/Al ratio increased by ca. 7%. These changes in the Si/Al ratio can be related to the structure stability of the aluminosilicate framework against the high-temperature treatment in ammonia.[4,12] As expected, after the nitridation treatment, the materials contain a high amount of nitrogen, in the 4-8 wt %.

Conclusions

Simple route for the synthesis of aluminosilicate micro/mesoporous composite materials via crystallization process followed by nitridation process been presented in this present study. Typically, the synthesis procedure involved the preparation of a mesostructured material composed of zeolite aluminosilicate micro/mesoporous material by a two-step crystallisation process. By varying the time allowed for the crystallisation of the precursor zeolite species (in the 2 – 16 range), materials with a variety of physico-chemical characteristics been obtained. Thus, for the shortest (2 h) and larger aging times (8 - 16h) composite materials consisting of a cubic MCM-48 phase and ZSM-5 zeolite been obtained. For intermediate aging time (3 - 6h), the zeolite phase disappears and the degradation of the cubic MCM-48 structure takes place. In general, the materials exhibit various levels of micro/mesoporous structure. Micro/mesoporous aluminosilica oxynitride materials were prepared by subjecting the zeolite aluminosilicate materials to a post synthesis treatment consisting of a high-temperature nitridation (i. e.

treatment with ammonia at elevated temperature). The textural properties of mesoporous aluminosilica oxynitride materials been found to be dependent on the nitridation conditions.

References

1. Z. Yang, Y. Xia, and R. Mokaya, Adv. Mater., 2004, 16, 727.
2. N. Alam and R. Mokaya, J. Mater. Chem., 2008, 18, 1383.
3. Y. Xia and R. Mokaya, J. Mater. Chem., 2004, 14, 863.
4. Y. Xia and R. Mokaya, J. Phys. Chem. C 2008, 112, 1455.
5. A. Sayari, P. Liu, M. Kruk and M. Jaroniec, Chem. Mater., 1997, 9, 2499.
6. M. Kruk, V. Antochshuk, and M. Jaroniec, J. Phys. Chem. B, 1999, 103, 10670.
7. S. A. Yousaf, and S. Ali, J. Faculty of Engineering and Technology, 2007-2008, 11.
8. Y. Xia, and R. Mokaya, Angew. Chem., Int. Ed. 2003, 42, 2639.
9. Y. Xia, and R. Mokaya, J. Mater. Chem. 2004, 14, 2507.
10. K. S. W. Sing, D. H. Everett, R. A. W. Haul, L. Moscou, R. A. Pierotti, J. Rouquerol, and T. Siemieniewska, Pure & Appl. Chem, 1985, 57, 603.
11. Z. Yang, Y. Xia, X. Sun, and R. Mokaya, J. Phys. Chem. B, 2006, 110, 18424.
12. Y. Xia, and R. Mokaya, J. Phys. Chem. B, 2003, 107, 6954.
13. J. Bernstein, G. R. Desiraju, J. R. Helliwell, T. Mak, P. Müller, P. Paufler, H. Schenk, P. Spadon, and D. Viterbo, The Basics of Crystallography and Diffraction, 3th eds, Oxford University press, UK, 2009, PP. 192-202.
14. V. K. Pecharsky and P. Y. Zavalij, Fundamentals of Powder Diffraction and Structural Characterization of Materials 2nd eds, Springer Science + Business Media, LLC, New York, USA, 2009, PP. 263-299.
15. P. Gabbott, Principles and Applications of Thermal Analysis, Blackwell Ltd, Oxford UK, 2008, PP. 87-163.
16. C. Guan, K. Wang, C. Yang, and X. S. Zhao, Microporous and Mesoporous Materials, 2009, 118, 503.
17. M. Sevilla, N. Alam, and R. Mokaya, J. Phys. Chem. C, 2010, 114, 11314.

5/24/2018